Weierstraß-Institut
für Angewandte Analysis und Stochastik

im Forschungsverbund Berlin e.V.

Preprint ISSN 0946 – 8633

New Slip Regimes and the Shape of Dewetting Thin Liquid Films

R. Konrad[1], K. Jacobs[1], A. Münch[2,3], B. Wagner[2], T. P. Witelski[4]

[1] Department of Experimental Physics, Saarland University, 66041 Saarbrücken, Germany
[2] Weierstrass Institute for Applied Analysis and Stochastics, Mohrenstr. 39, 10117 Berlin, Germany
[3] Institute of Mathematics., Humboldt University Berlin, 10099 Berlin, Germany
[4] Department of Mathematics, Duke University, Durham, NC 27708-0320, USA

submitted: December 17, 2004

No. 993
Berlin 2004

1991 *Mathematics Subject Classification.* 76D08, 76E17, 74A55.

Key words and phrases. slippage, lubrication approximation, interfacial instability.

Edited by
Weierstraß-Institut für Angewandte Analysis und Stochastik (WIAS)
Mohrenstraße 39
10117 Berlin
Germany

Fax: + 49 30 2044975
E-Mail: preprint@wias-berlin.de
World Wide Web: http://www.wias-berlin.de/

Abstract

We compare the dewetting behavior of liquid polymer films on silicon/silicon oxide wafers that have been coated with either Octadecyltrichlorosilane (OTS) or Dodecyltrichlorosilane (DTS). Our experiments show that the dewetting rates for DTS are significantly larger than for OTS. We also compare the profile of the rim that forms as the film dewets and find that it develops a spatially decaying oscillatory structure on the side facing the undisturbed film if an OTS coated wafer is used, but is monotonically decaying for DTS. We argue that for this situation only the solid/liquid friction coefficient can be different, suggesting that slippage plays a role in this transition. For the first time, we show here that this transition is in fact captured by a lubrication model that can be derived from the Navier-Stokes equations with a Navier-slip boundary condition at the liquid/solid interface, and accounts for large slip lengths.

Thin films of liquid polymers play an important role in numerous technological processes ranging from lithography to biological membranes [13]. In recent years, one major focus of interest has been to understand the dynamics and morphology of polymer films dewetting from hydrophobic substrates. The film thickness typically ranges on the scale of tens to a few hundred nanometers. Dewetting starts by the formation of holes due to spinodal decomposition or heterogeneous nucleation. As the holes grow, the displaced liquid collects in growing rims surrounding the holes.

Many studies have focused on this dynamics following rupture, e.g. on the appearence of a rim, or on the presence or vanishing of a damped oscillatory structure that joins the rim to the external undisturbed film. Concerning the latter problem the authors of Refs. [15, 6, 18] proposed to include viscoelastic effects into their model in order to explain the profiles of the monotonically decaying rims that were experimentally observed for longer chained polymer films [14]. In Ref. [16] shear-thinning properties of the polymer film were included to explain such differing morphologies. In this letter we concentrate on the rim morphology affected by slippage. The occurence and the nature of slippage of liquids on solid surfaces is vividly discussed in the literature [2, 3], and is of large technological interest since a sliding fluid can flow faster through e.g. microfluidic devices.

We present here new experiments that investigate the dewetting dynamics and morphology of thin films of atactic polystyrene of low molecular weight on oxidized Si wafers. To change the boundary condition at the solid/liquid interface without influencing the contact angle, the wafers are coated with either a monolayer of Octadecyltrichlorosilane (OTS) or with Dodecyltrichlorosilane (DTS), while keeping all

other properties of the substrate and the liquid fixed. Hence we can study directly the influence of slippage on the dewetting dynamics.

Our experiments show that if OTS is used the shape of the rim develops a damped oscillatory structure towards the undisturbed film, while for a DTS coating the rim decays monotonically. A clue to an explanation for this surprising behaviour is provided by a comparison of the dewetting rates, which are markedly higher for DTS, indicating a lower friction coefficient, and hence higher slippage, for this type of coating.

We develop a mathematical model that is able to predict these experimental findings on the basis of purely viscous and slippage effects. This model can be derived from the Navier-Stokes equations together with the Navier-slip boundary condition. Making use of the scale separation between the height of the film H and the lateral dimension of the rim L, we then find two distinguished limits that lead to two different lubrication models, depending on the order of magnitude of the slip length. The slip length can be understood as the length below the solid/liquid interface where the velocity extrapolates to zero, [1, 9]. For a slip length that is small, or at most of the order of the thickness of the dewetting film, we obtain the well-known lubrication equation [13]. When the slip length is assumed to be much larger than the thickness of the film, we obtain a different lubrication model consisting of a system of equations for the profile and the velocity of the film. We show that this second model captures the disappearance of the capillary waves behind the rim for sufficiently large slip length, which compares well with our experimental results. This suggests that for many micro-fluidic flows slip effects may dominate the dynamics and control morphological instabilities that occur in dewetting.

The liquid used in our experiments was atactic polystyrene (PS) with a molecular weight of 13.7 kg/mol (polydispersity $M_w/M_n = 1.03$). The samples were prepared by spin casting a toluene solution of PS onto mica, floating the films on Millipore^{TM} water, and then picking them up with our wafers. We used two different silane coatings of the Si wafer (2.1 nm native oxide layer), Octadecyltrichlorosilane (OTS) and the shorter Dodecyltrichlorosilane (DTS), respectively, prepared by standard techniques [20]. The thicknesses of these self-assembled monolayers measured by ellipsometry are 2.2 nm for OTS and 1.5 nm for DTS. Surface characterization by scanning probe microscopy (SPM) revealed a RMS roughness of 0.09(1) nm (OTS) and 0.13(2) nm (DTS), and a static contact angle of polystyrene droplets of $68(2)^o$ and $66(2)^o$, respectively. The effective interface potential of a polystyrene film of thickness h on OTS and DTS covered Si wafers, which is defined as the excess free energy it takes to bring the two interfaces from infinity to the certain distance h, cf. Refs. [4, 17], is given by

$$\phi(h) = \frac{c_s}{h^8} - \frac{A_{SAM}}{12\pi h^2} + \frac{A_{SAM} - A_{SiO}}{12\pi(h + d_{SAM})^2} + \frac{A_{SiO} - A_{Si}}{12\pi(h + d_{SAM} + d_{SiO})^2}\,. \tag{1}$$

Here, additivity of the van der Waals forces is assumed which has proven to be

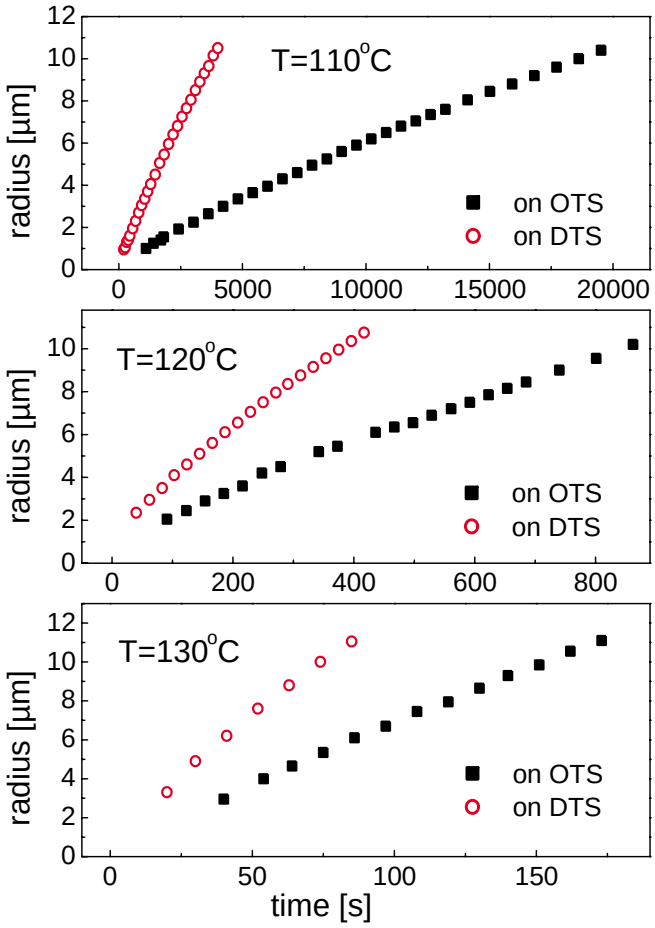

Figure 1: The growth of hole radii of dewetted regions as a function of time on OTS/DTS substrates at three different temperatures.

successful [18]. The Hamaker constants of PS on Si, on SiO and on the self assembled monolayers are $A_{Si} = -1.4(6) \cdot 10^{-19}$ J, and $A_{SiO} = A_{SAM} = 2.2(4) \cdot 10^{-20}$ J [18]. Using the relation $\phi(h_m) = \sigma(\cos\theta - 1)$ between the depth of the global minimum of ϕ and the contact angle θ and the surface tension of polystyrene, $\sigma = 30.8$ mN/m, we obtain a short-range repulsion strength $c_s = 1.8(4) \cdot 10^{-81}$ J/m^6. All polystyrene films in this study are 130(5) nm thick. To induce dewetting, the films were heated to three different temperatures (110^{o}C, 120^{o}C, 130^{o}C) above the glass transition temperature of PS (93^{o}C). After a few seconds circular holes appear due to heterogeneous nucleation and grow rapidly [7]. The radii of the emerging holes in the PS(13.7k) film were measured by optical microscopy. As shown in Fig. 1, dewetting progresses more quickly on DTS than on OTS coated substrates.

After quenching the samples to room temperature, we measured the glassy rim profiles by SPM (Multimode, Digital Instruments, Santa Barbara, USA) in Tapping Mode^{TM} (Fig. 2). To guarantee that the rim does not change shape while cooling we also scanned liquid profiles, but could not detect any difference in shape. To

ensure consistency, all rim profiles were taken of holes of about identical diameter, 22 μm.

Fig. 2 demonstrates that the type of substrate affects the rim profile: On OTS covered substrates, the rim of the dewetting PS film exhibits an oscillatory shape, whereas on DTS covered surfaces, at the same temperature, no oscillation is observed. The inset to Fig. 2a) clarifies the oscillatory rim shape on OTS by plotting $|h(x) - H|$ in a semilog plot for 120^{o}C, where H denotes the initial thickness of the film. To account for the influence of viscosity, we compare the results on DTS and on OTS for three different dewetting temperatures, cf. Fig. 2b) and c), respectively. On DTS we are able to induce an oscillatory shape for 130^{o}C.

We explain these results as follows. At the same temperature the liquids on both samples have exactly the same properties: the viscosity μ as well as the surface tension σ do not depend on the substrate underneath. Additionally, the contact angle of polystyrene on both surfaces is constant within the experimental error. Therefore, the spreading coefficient $S = \sigma(1 - \cos\theta)$ that is the driving force of the dewetting process is identical for OTS and DTS. The only parameter that could be changed is the friction coefficient at the solid/liquid interface. The friction coefficient indeed can be changed, for instance, by the use of polymer brushes as has been shown [2]. Since we observe a clear difference in the dewetting velocity, this friction coefficient and with it the magnitude of slippage has to be affected by the different coatings, i.e. we expect slippage of PS(13.7k) on DTS to be significantly larger than on OTS.

We introduce a theoretical model describing this dewetting scenario by taking into account large variations of slip. We start with the 2D Navier-Stokes equations for viscous incompressible Newtonian flow and assume that for holes whose radii are large compared to the width of the rim, the influence of the rim curvature is weak and can be neglected,

$$\begin{aligned} \rho\,(\partial_t \mathbf{u} + \mathbf{u}\cdot\nabla\mathbf{u}) &= -\nabla(p + \phi(h)) + \mu\nabla^2\mathbf{u}\,, \\ \nabla\cdot\mathbf{u} &= 0\,. \end{aligned} \tag{2}$$

Here, $\mathbf{u} = (u, w)$ is the velocity, ρ the density, μ the viscosity of the liquid and p the pressure. For the 2D free surface flow we have the usual normal and tangential stress conditions at the free surface and the kinematic condition $\partial_t h = w - u\partial_x h$ for the film thickness $z = h(x, t)$. On the solid surface we have impermeability $w = 0$ and a Navier-slip condition $u = b\,\partial_z u$, where b is the slip length. We nondimensionalize $(z^*, h^*, b^*) = (z, h, b)/H$ and $x^* = x/L$, where L is the typical lateral scale of the dewetting rim, with $\varepsilon = H/L \ll 1$. Similarly $(u^*, \varepsilon w^*) = (u, w)/U$, $(p^*, \phi^*) = (p, \phi)/P$, $t^* = \varepsilon U/Ht$, where $P = \mu U/(\varepsilon H)$, $U = \sigma\varepsilon^3/\mu$ with σ being the constant surface tension. If the dimensionless slip length $b \sim O(1)$, we obtain, to leading order in ε, the lubrication equation $\partial_t h = -\partial_x\left[(h^3/3 + bh^2)\,\partial_x\left(\partial_x^2 h - \phi'(h)\right)\right]$ for weak slippage, where we have dropped the stars. However, for this model, the rims always have a spatially oscillatory shape as is known from previous investigations [19].

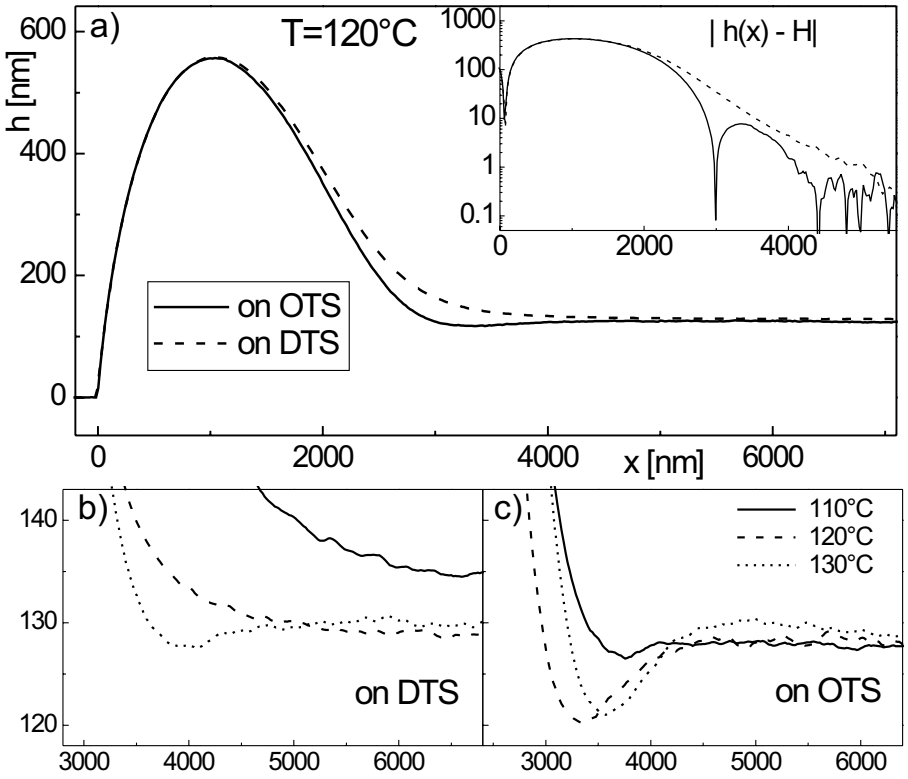

Figure 2: Rim profiles of 130 nm PS films on DTS and OTS covered Si wafers a) at constant temperature (the inset depicts a semilog plot of $|h(x) - H|$), b) and c) at three different temperatures on DTS and OTS surfaces, respectively. Profiles are shown with the three-phase contact-line shifted into the origin.

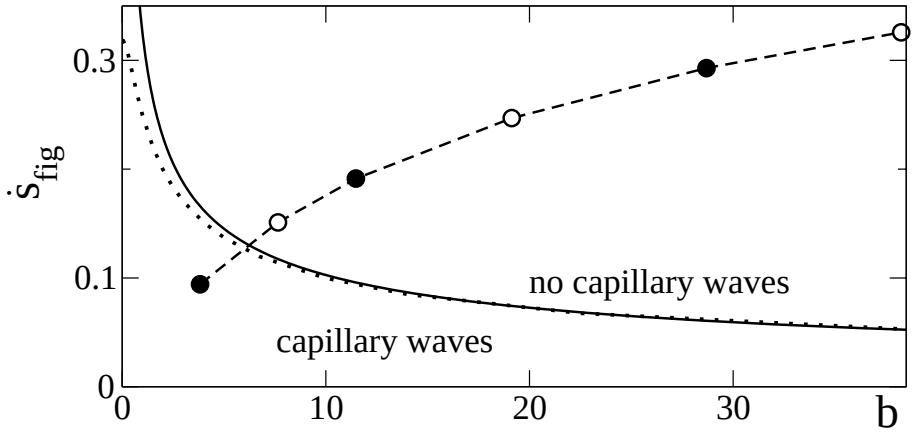

Figure 3: Transition curves in $(b, \dot{s}_{\rm fig})$ parameter space for profiles with to without capillary waves, calculated from the lubrication model (solid line) and Stokes model (dotted line). The dashed line shows the contact-line speed for different slip lengths, calculated from the lubrication model.

If, however, the slip length is large, we rescale the velocity as $u = b\tilde{u}$ and time as $t = \tilde{t}/b$, i.e. in effect scaling the velocity scale U with b. We then find a regime of $b = \beta/\varepsilon^2$, which yields a different lubrication model (dropping the tildes)

$$\partial_t h + \partial_x(h\,u) = 0\,, \tag{3}$$

$$\beta \mathrm{Re}\,(\partial_t u + u\,\partial_x u) = \frac{4\beta}{h}\partial_x\,(h\partial_x\,u) + \partial_x\left(\partial_x^2 h - \phi'(h)\right) - \frac{u}{h}\,, \tag{4}$$

with Re=$\rho\sigma H/\mu^2$. The two models we have introduced so far are embedded in a whole family of lubrication models that can be derived for different regimes of the slip length. They are in fact distinguished limits, in the sense that they are richer in structure than the other regimes and depend explicitly on the slip length. The other regimes are the no-slip regime, the intermediate regime and the lubrication model describing retracting free foam films. The intermediate regime is obtained for slip lengths of order $b = \beta/\varepsilon$. It also arises from (3)–(4) in the limit $\beta \to 0$, which yields a scalar lubrication equation with an h^2 mobility. Some recent results on the contact-line instability of dewetting thin films in this regime can be found in Ref. [11]. The model for retracting free foam films, see [5], is recovered by rescaling u with β and then letting $\beta \to \infty$. This regime corresponds to $b \gg \beta/\varepsilon^2$. A more detailed derivation of all these regimes from the Navier-Stokes equations, asymptotic analysis and comparison to numerical results can be found in Ref. [12]. A similar derivation of the lubrication models has just appeared in Ref. [8].

We seek an approximate description of the portion of the profile of the dewetting rim that connects to the undistributed uniform film $h = 1$ for $x \to \infty$. Consistency with Eqs. (3) and (4) requires that $u \to 0$ as $x \to \infty$. It is convenient to shift to a comoving frame of reference $\xi = x - s(t)$, where $s(t)$ denotes the position of the

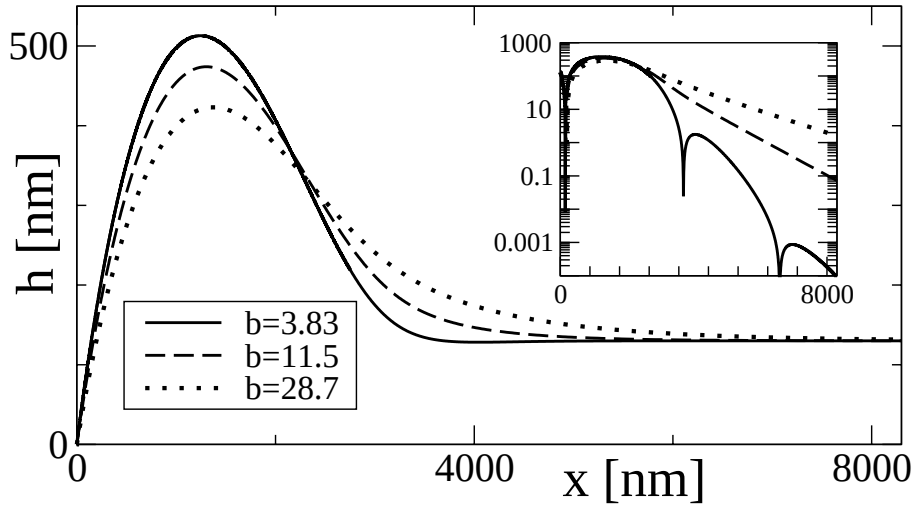

Figure 4: Rim profiles for different slip lengths b non-dimensionalized with $H = 130\,\mathrm{nm}$. The inset shows a semilog plot of $\max(|h(x) - H|,\, 10^{-5})$.

contact line. Near the flat state, the evolution can be described by introducing the ansatz $h(x,t) = 1 + \delta\varphi(\xi)\,, \quad u = \delta v(\xi)\,, \quad \delta \ll 1$, into Eqs. (3) and (4). Keeping only the $O(\delta)$ terms yields

$$-\dot{s}^2\beta\,\mathrm{Re}\partial_\xi\varphi = 4\dot{s}\beta\partial_\xi^2\varphi + \partial_\xi^3\varphi - \dot{s}\varphi\,. \tag{5}$$

We have to note here that we neglect the effect of the slowly growing rim. The normal mode solutions $\varphi(\xi) = e^{\omega\xi}$ of (5), which decay for $\xi \to \infty$ are spatially oscillating due to a pair of complex conjugate ω, if the discriminant corresponding to the dispersion relation for ω

$$D = \frac{4\dot{s}^4\beta^3}{3^3}\,(\mathrm{Re} - 4\beta)\,\mathrm{Re}^2 + \frac{8\beta^2\dot{s}^2}{3}\mathrm{Re} - \frac{4^4\beta^3\dot{s}^2}{3^3} + 1 \tag{6}$$

from the dispersion relation is positive. Hence, the rim passes over into a damped capillary wave. But if it is negative the complex conjugate ω is replaced by two real modes, which allows the solution $\varphi(\xi)$ to decay monotonically for $\xi \to \infty$. In our case the Re number is extremely small and can be neglected, so that the transition from complex conjugate to real decaying modes occurs when $\beta > \beta_{th}(\dot{s}) = (3/4)/(4\dot{s}^2)^{1/3}$. Equivalently, this can be written as $b_{th} = (3/4)^3\,/(4\dot{s}_{\mathrm{fig}}^2)$, where $\dot{s}_{\mathrm{fig}} = \varepsilon^3\dot{s}^*$ is the contact-line velocity nondimensionalized with σ/μ. This threshold is shown in Fig. 3. The transition from complex conjugate to real decaying modes can also be found from the full Stokes equation. In Fig. 3 we also show the corresponding threshold that was numerically obtained from the normal mode solution of the linearized Stokes problem. The figure shows that they compare well except for small slip lengths.

The diagram in Fig. 3 allows predictions regarding the shape of the dewetting ridge only if both the dimensionless slip length b and speed $\dot{s}_{\mathrm{fig}}$ of the wave are known. The

contact-line speed depends on the slip length and can be obtained from simulations of dewetting fronts using Eqs. (3) and (4). The dashed line shows the value for the dewetting rate when the cross sections of the rims have the same area as those found in our experiments. The values of the slip length that were used in the simulations for the three profiles shown Fig. 3 are the same as for the filled circles in Fig. 4.

One observes that as b is increased, the dewetting rate increases and for slip lengths larger than about six, the dashed line in Fig. 3 leaves the region where capillary waves are expected. Indeed, the profiles in the simulations show a dip for the smallest $b = 3.83$, but monotone profiles for the other b-values, which are larger than six. Closer inspection of the profile in a semilog plot of the profile shows a second maximum for the smallest b, indicating that we have the oscillatory structure of a wave, which however decays very rapidly for increasing x.

We finally note that, since the contact angles here are not small, it is reasonable to compare our results using the linearized curvature in Eq. (4) with those, where the fully nonlinear curvature is accounted for, in a similar fashion as done e.g. in [10]. We found from our simulations that in this case only the dewetting rates for large b are affected in that they are modestly decreased; the profiles however, remain very close to those presented above.

Comparing now the theoretical results with the experimental observations, we find them in good qualitative agreement: At $T = 120^o$C, a dip is only seen in the ridge on the OTS coated wafer, where slippage is smaller according to the dewetting rates than for the DTS coated wafer. Repeating the experiment at lower and higher temperature confirms this trend that the oscillations are suppressed, i.e., smaller or even absent, on the DTS wafer. The linearized analysis and the numerical computations for the film profiles show the same behaviour: Increasing the slip length for otherwise fixed parameters suppresses the spatially oscillatory structure on the side of the rim facing the undisturbed film.

To conclude, we have shown that the transition from an oscillating to a monotonically decaying dewetting rim profile that has been observed for the first time by solely changing the friction at the substrate can be captured by a lubrication model for Newtonian liquid in a regime of large slip lengths.

Acknowledgements

AM acknowledges support via DFG grant MU 1626/3-1 and by the DFG research center Matheon, Berlin. RK and KJ acknowledge support by grant JA 905/3-1 within the DFG priority program 1164, and generous support by Siltronic AG, Burghausen, Germany. TW is grateful for the hospitality of WIAS and HU and was supported by NSF grants #0244498 and #0239125.

References

[1] F. Brochard-Wyart, C. Gay, and P.G. de Gennes. Slippage of polymer melts on grafted surfaces. *Macromolecules*, 29:377–382, 1996.

[2] L. Bureau and Léger. Dewetting of supported viscoelastic polymer films: Birth of rims. *Langmuir*, 20:4523, 2004. and references therein.

[3] P.G. de Gennes. Wetting: Statics and dynamics. *Review of Modern Physics*, 57:827, 1985.

[4] S. Dietrich. In *Phase Transitions and Critical Phenomena*, editor, C. Domb and J.L. Lebowitz. Academic, London, Vol. 12, 1988.

[5] T. Erneux and S. H. Davis. Nonlinear rupture of free films. *Phys. Fluids*, 5:1117, 1993.

[6] S. Herminghaus, R. Seeman, and K. Jacobs. Generic morphologies of viscoelastic dewetting fronts. *Phys. Rev. Let.*, 89:56101, 2002.

[7] K. Jacobs, S. Herminghaus, and K. R. Mecke. Thin liquid polymer films rupture via defects. *Langmuir*, 14:965–969, 1998.

[8] K. Kargupta, A. Sharma, and R. Khanna. Instability, dynamics and morphology of thin slipping films. *Langmuir*, 20:244–253, 2004.

[9] L. Léger. Friction mechanisms and interfacial slip at fluid-solid interfaces. *J. Phys.: Condens. Matter*, 15:S19–S29, 2003.

[10] A. Münch. Dewetting rates of thin liquid films. Journal of Physics: Condensed Matter, accepted, 2004.

[11] A. Münch and B. Wagner. Contact-line instability of dewetting thin films. Physica D, accepted, 2004.

[12] A. Münch, B. Wagner, and T.P. Witelski. Dewetting slip regimes. in preparation.

[13] A. Oron, S. H. Davis, and S. G. Bankoff. Long-scale evolution of thin liquid films. *Review of Modern Physics*, 69(3):931–980, 1997.

[14] G. Reiter. Dewetting of highly elastic thin polymer films. *Phys. Rev. Let.*, 87:186101, 2001.

[15] S. A. Safran and J. Klein. Surface instability of viscoelastic thin flims. *J. Phys. II France*, 3:749–757, 1993.

[16] F. Saulnier, E. Raphaël, and P. G. de Gennes. Dewetting of thin film polymers. *Phys. Rev. E.*, 66:061607, 2002.

[17] M. Schick. In *Liquids and Interfaces*, editor, J. Charvolin et al., . Elsevier Science, Amsterdam, 1989.

[18] R. Seemann, S. Herminghaus, and K. Jacobs. Dewetting patterns and molecular forces: A reconciliation. *Phys. Rev. Let.*, 86(24):5534–5537, 2001.

[19] R. Seemann, S. Herminghaus, and K. Jacobs. Shape of a liquid front upon dewetting. *Phys. Rev. Let.*, 87:196101, 2001.

[20] S.R. Wasserman, S. R. Y.-T. Tao, and G. M. Whitesides. Structure and reactivity of alkylsiloxane monolayers formed by reaction of alkyltrichlorosilanes on silicon substrates. *Langmuir*, 5:1074–1087, 1989.